Applied Surface Science 295 (2014) 54–58

Contents lists available at ScienceDirect

Applied Surface Science

journal homepage: www.elsevier.com/locate/apsusc

Helium diffraction study of pentacene films on Au(1 1 1)

E. Albayrak[a], M.F. Danışman[b,*]

[a] Department of Materials and Metallurgical Engineering, Ahi Evran University, Kırşehir 40000, Turkey
[b] Department of Chemistry, Middle East Technical University, Ankara 06531, Turkey

ARTICLE INFO

Article history:
Received 2 September 2013
Received in revised form 1 January 2014
Accepted 2 January 2014
Available online 13 January 2014

Keywords:
Pentacene
Organic semiconductors
Helium diffraction
Supersonic molecular beam deposition
Au(1 1 1) surface
Quartz crystal microbalance
Quartz crystal resonance frequency shift

ABSTRACT

Here we present a helium atom diffraction study of pentacene films on Au(1 1 1) surface prepared by supersonic molecular beam deposition. Though investigated parameter space was limited no significant difference between the films prepared by different deposition energies was observed. Completion of monolayer coverage was confirmed by simultaneous helium scattering and quartz crystal resonance frequency shift measurements during pentacene film growth on the gold electrode of a quartz resonator. Monolayer films were found to adopt a (6×3) unit cell which was also observed for pentacene monolayers on Ag(1 1 1). However no ordered multilayer film structure could be observed which is in contrast with the previous Ag(1 1 1) studies.

1. Introduction

Organic electronics is continuing to attract very intense research efforts thanks to new type of organic materials and technologies that help utilizing the potential advantages of these systems such as reduced cost, flexibility and controlled functionalization [1–4]. Pentacene, which is one of the most promising small molecule organic semiconductors, is also enjoying attention due to its use in field effect transistors [1,2,5]. Though many basic properties and limits of pentacene and devices that employ pentacene have been well established, there are still issues open to development and further investigation. One such aspect of pentacene TFTs is the charge injection from/to the metal electrodes to/from the organic semiconductor over the interface between the SiO_2 channel region and the metal electrode. Since the performance of a TFT depends on, among the other factors, the efficiency of charge injection, understanding and controlling structural and electronic properties of pentacene films on metal surfaces, such as gold, that constitute electrode material in TFTs is a very important subject both for device fabrication and fundamental science.

Pentacene films on metal surfaces like gold, silver and copper have been studied in detail [6–27] and it has been shown that they form a first layer with lying down molecules [6–8,10,11,23,27,28]. The second and higher layers were shown to adopt bulk like structures [10,11,20,27,28]. On Au(1 1 1), pentacene was shown to form several different unit cell structures as a function of coverage by means of scanning tunneling microscopy [6,7,11]. However structure of pentacene films on Au(1 1 1) have not been studied by diffraction techniques. In the past we studied pentacene films grown by supersonic molecular beam deposition (SMBD) on Ag(1 1 1) surfaces and showed that increasing the energy of the deposited molecules increases the quality of the films [10,27,29]. By using helium atom diffraction for characterizing the films and deducing the film coverage from the specular reflection intensity level we were able to show that the first pentacene monolayer (ML) on Ag(1 1 1) was made up of a (6×3) unit cell with lying down molecules. In addition we were able to grow ordered pentacene overlayers for high energy pentacene molecules at 200 K substrate temperature. At higher or lower substrate temperatures we observed deterioration in the multilayer film quality. In order to contribute to the understanding of crystal structure of pentacene films on Au(1 1 1) surfaces here we extended our helium atom diffraction measurements to Au(1 1 1) surfaces. In addition, to correlate helium specular reflection intensity level to film coverage, here we grew pentacene films on the gold electrode surface of a quartz crystal oscillator which enabled us to monitor film coverage by helium scattering and resonance frequency shift measurements simultaneously. For the first ML we observed a (6×3) diffraction pattern which did not change significantly with deposition energy. However no ordered multilayer film structure could be observed which is in contrast with our previous Ag(1 1 1) studies.

* Corresponding author at: Department of Chemistry, Middle East Technical University, Ankara 06800, Turkey. Tel.: +90 0 312 2107618; fax: +90 0 312 2103200.
E-mail address: danisman@metu.edu.tr (M.F. Danışman).

0169-4332/$ – see front matter © 2014 Elsevier B.V. All rights reserved.
http://dx.doi.org/10.1016/j.apsusc.2014.01.003

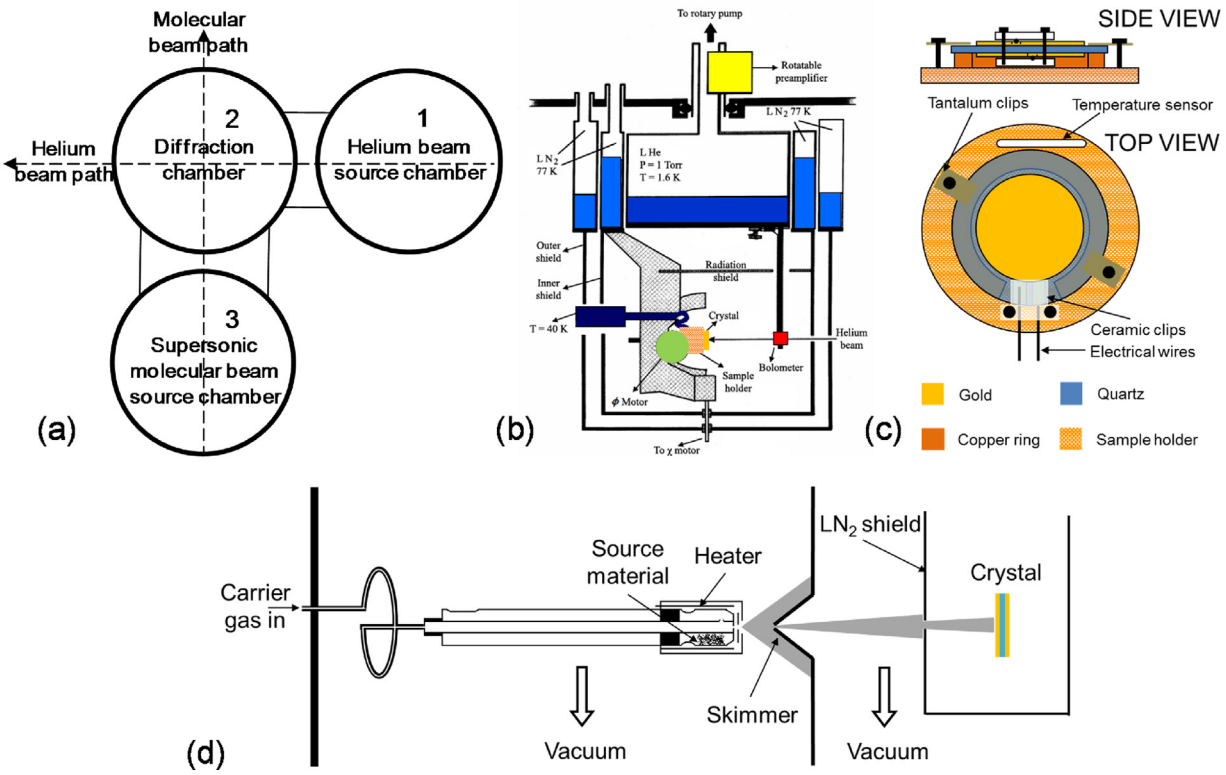

Fig. 1. Schematic of the experimental system (a), diffraction chamber (b), quartz crystal resonator mounting (c) and the supersonic molecular beam source (d).

2. Experimental methods

Pentacene films were grown by using a supersonic molecular beam deposition (SMBD) source which is shown schematically in Fig. 1 and which was detailed before [10,27]. Basically, in SMBD, the organic material is mixed in a carrier gas and the mixture is expanded into vacuum through a micro nozzle. The resulting supersonic beam of the organic material is then sent to the substrate surface for coating. During the studies that will be discussed here 200 K substrate temperature was used since in our past studies on pentacene on Ag(1 1 1) we found the optimum substrate temperature for an ordered multilayer film growth to be 200 K as mentioned in the introduction above. Under the standard SMBD source working conditions pentacene kinetic energies were determined before by time of flight measurements as 2.2 eV for helium carrier gas. [27] Though we do not have a conventional thermal evaporator (i.e., organic molecular beam deposition source) in our system, to simulate the low energies relevant in conventional thermal evaporation we used krypton carrier gas in our SMBD source which results in a pentacene kinetic energy of 0.2 eV (which is still somewhat larger than the energies relevant in conventional thermal evaporation sources). [27]

The grown films were monitored in real time by using a low energy atom diffraction (LEAD) setup which is attached to the SMBD source as shown in Fig. 1. The details of LEAD setup was also discussed before and here only basics will be explained [10]. For LEAD measurements a mono-energetic helium beam (14 meV with velocity dispersion of 2%) was scattered form the sample surface and the angular variation of the scattering intensity was measured by using a liquid helium cooled bolometer detector. Due to reduced sensitivity of the detector and the increased inelastic scattering with increasing temperature, diffraction data was recorded at 60–80 K surface temperature. However specular reflection intensity (SRI) can be measured up to 600 K surface temperature. The angular data were converted to momentum space by using the equation $\Delta K_{//} \acute{Y} = k_i(\sin\theta_f - \sin\theta_i)$ where $\Delta K_{//}$ is the parallel momentum transfer, and θ_i and θ_f are the incident angle and the detector angular position, respectively. For the measurements reported here θ_i was ≈57° and θ_i was scanned from −15° to 75°. Our apparatus has a resolution function which depends on both θ_i and θ_f and the corresponding instrument limited diffraction peak widths vary from 2° (at $\theta_f = -15°$) to 0.8° (at $\theta_f = 75°$). The finite domain size of the diffracting film increases the peak widths further and in turn, for instance, a 50 Å domain produces a diffraction peak of width 2.3° (corresponding to 0.2 $Å^{-1}$ reciprocal space width) at $\theta_f = 0°$ (corresponding to $\Delta K_{//} = -4.2\ Å^{-1}$) [30].

A unique future of our setup is that as the sample surface (substrate), metal electrode surface of a quartz crystal oscillator can be used [31]. Hence LEAD and quartz crystal resonance frequency shift (QRFS) measurements can be performed simultaneously while the film is grown by SMBD. For QRFS measurements a 6 MHZ, polished AT cut crystal with 0.28 mm thickness provided by International Crystal Manufacturing (ICM) was installed in the LEAD setup sample holder as depicted in Fig. 1. Gold electrode films on the quartz oscillator were grown by thermal evaporation and had a SRI of as high as 10% of the incident helium beam intensity, after sputter-anneal cleaning. The quartz oscillator was driven and the resonance frequency shift was measured using a frequency modulation technique which was described before [31,32]. According to Sauerbrey equation [33] the shift in the resonance frequency of a quartz oscillator, Δf, can be given as $\Delta f = -\frac{2f_{res}^2}{nZ_q}\frac{m}{A}$, where f_{res} is the resonance frequency, Z_q is the acoustic impedance of the quartz crystal, m is the mass of the adsorbed material, A is the area of the electrodes and n is the overtone number (which is 1 here since first overtone was used).

When QRFS measurements were not required the film growth was performed on a single crystal gold surface to increase the helium scattering intensity. For such measurements a Au(1 1 1) surface with an orientation accuracy of <0.1° (purchased from Mateck

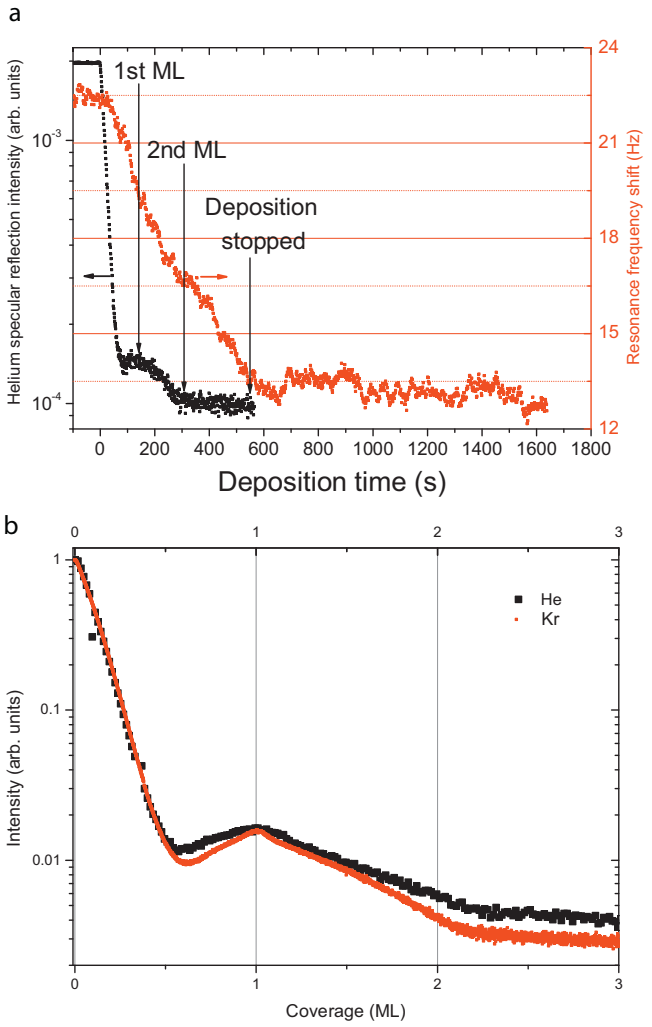

Fig. 2. (a) Helium SRI (black trace) and QRFS (red trace) as a function of pentacene deposition time on the gold electrode surface of a quartz oscillator. Deposition was performed with helium carrier gas. (b) Normalized helium SRI as a function of coverage for pentacene deposition on single crystal Au(1 1 1) surface with different carrier gasses. (For interpretation of the references to colour in this figure legend, the reader is referred to the web version of this article).

GmbH) was used. Before each experiment, the surface was treated with several sputter–anneal cycles and the cleanliness was confirmed by observation of the gold reconstruction diffraction peaks and a SRI of no less than 25% of the incident beam.

3. Results and discussion

In Fig. 2a, SRI and QRFS data, recorded while pentacene is grown by helium carrier, is shown. As can be seen, before deposition both SRI and QFRS values are constant, whereas with the starting of the deposition both start to decrease. Since SRI is very sensitive to surface corrugation and the adsorbates have a very large cross section for helium scattering, with increasing coverage there is a very large decrease in the SRI signal. However once the monolayer start to complete, at about 150 s, the cross sections of the adsorbates (pentacene molecules) start to overlap and the scattering helium atoms feel a smother surface corrugation and the SRI signal recovers partially. Once the second layer starts to form the surface corrugation increases and the SRI starts to decrease again. After 300 s of deposition however SRI reaches a stable value probably because the surface corrugation does not change considerably with increasing coverage till deposition was stopped at about 600 s. When the QRFS data is examined it can be seen that at 150 s the shift is 3 Hz (from 22.5 Hz to 19.5 Hz), at 300 s 6 Hz and at the end of the deposition 9 Hz. QRFS was continued to be monitored after the end of the deposition and it was constant within the noise level of our setup. To deduce a film thickness form the QRFS data the density of the pentacene film should be known to be used in the Sauerbrey equation. As will be discussed later, from the diffraction data we found that pentacene has (6×3) unit cell on the Au(1 1 1) surface which has mass density of 3.56×10^{-7} kg/m^2. Hence, a single ML of pentacene can be calculated to cause a shift of −2.91 Hz in the resonance frequency of the quartz oscillator which is very close to what we observed in our measurements as discussed above. Though using gold electrode surface of the quartz oscillator as the substrate was necessary for correlating helium SRI to film coverage through QRFS data, due to poor quality of such gold surfaces helium scattering intensity is not high enough for reliable scattering measurements. In addition since such gold surfaces are made up off Au(1 1 1) terraces oriented randomly with respect to each other, they are not appropriate substrates for determining the crystal structure of overlaying films. Hence, we continued our studies with single crystal Au(1 1 1) surfaces.

In Fig. 2b normalized helium SRI as a function of pentacene surface coverage is shown for pentacene films grown by using helium and krypton carrier gasses. The coverage values in this plot are calculated by associating 1 ML coverage to SRI recovery maximum point. As discussed above with increasing coverage SRI decreases and with completion of the first ML a recovery peak is observed. Following this peak SRI decreases again till a stable and low SRI level is achieved due to formation of a highly corrugated surface at high coverages (>2 ML). The SRI behavior is almost identical for both helium and krypton gasses indicating a similar film formation mechanism unlike what we observed in the past for pentacene growth on Ag(1 1 1) surfaces.

Diffraction scans recorded at 60–80 K from the ML pentacene films (pentacene films corresponding to coverage at recovery peak maxima in Fig. 2b) are shown in Fig. 3. As can be seen there is no significant difference between the films grown by helium or krypton carrier gas. When the monolayer diffraction scans along different crystallographic directions (Fig. 3b) are examined it can be seen that pentacene ML follows the symmetry of underlying gold surface (i.e., diffraction scans along 0° and 60° azimuthal directions are identical). In addition diffraction peak positions are in agreement with (6×3) unit cell which was observed before on Ag(1 1 1) surface.

In Fig. 4a diffraction scan of a multilayer (MUL) film grown by helium carrier gas is shown (since krypton data was similar to helium data only diffraction scans of MUL films grown by helium are shown in Fig. 4). No specular reflection or diffraction peaks could be observed for MUL films either grown by helium or carrier gas. This indicates that the MUL films are disordered regardless of the type of the carrier gas. However when the MUL films are annealed some ordering and desorption was observed depending on the annealing temperature and MUL thickness. For instance, when the MUL whose diffraction scan is shown in Fig. 4a (black trace) is annealed to 400 K a considerable increase in specular reflection peak intensity was observed. However, there still were no discernable diffraction peaks. After a consecutive 450 K annealing specular reflection intensity increased further and diffraction peaks corresponding to (6×3) monolayer unit cell were observed. This indicates that during 450 K annealing desorption of multilayers takes place and some portion of the first monolayer becomes visible to the scattering helium atoms. However, it can be concluded that the desorption is not complete since, after the 450 K annealing, the SRI intensity is not as high as that of the 1 ML films (shown in Fig. 3) and the observed diffraction peaks are very broad. Desorption is also evidenced by the behavior of SRI as a function of substrate tem-

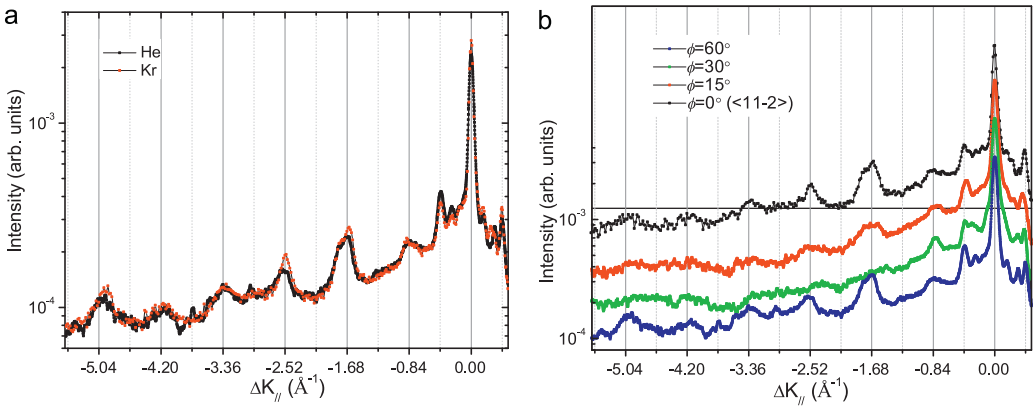

Fig. 3. (a) Helium diffraction scans along ⟨1 1 −2⟩ direction from pentacene MLs grown on Au(1 1 1) with different carrier gasses. Scans are recorded after deposition is stopped and the substrate temperature was reduced to 80 K. (b) Diffraction scans along different crystallographic directions from the pentacene ML grown by helium carrier gas. ⟨1 1 −-2⟩ direction was assigned the azimuthal angle of 0° arbitrarily as a reference.

perature which is shown in Fig. 4b for a 6 ML thick multilayer film. During heating of the MUL film the SRI decreases with increasing temperature due to increased inelastic scattering and decreasing detector sensitivity. However, between 380 K and 400 K an increase in the SRI could be observed which is due to desorption of the MULs that leave behind a smoother surface some of which is only covered by a monolayer. After the completion of desorption at 400 K, the SRI decreases again with increasing temperature. When the film is cooled the SRI intensity increases to a value much higher than its pre-annealing level. However we should here note that this desorption was not always observable and depends on the thickness of the multilayer film and how the annealing is performed (stepwise or not). Nevertheless the observed desorption temperature is in agreement with the previous studies on Ag(1 1 1) [10] and Au(1 1 1) [7] and the standard sublimation enthalpy of pentacene [34].

In previous STM studies at complete monolayer coverage an incommensurate film with unit cell dimensions of $a = 1.55 \pm 0.05$ nm, $b = 0.64 \pm 0.05$ nm, and $\gamma = 82.0 \pm 2^\circ$ and lateral density of 1.02×10^{14} molecules/cm^2 was observed by Kang and Zhu [11]. Similar structures were also observed by Parkinson and co-workers (denoted as "type B" and "type C" in their work) [6,7]. (6×3) unit cell found here, however, has a lower density (7.71×10^{13} molecules/cm^2) then these films and in addition it is commensurate with the underlying substrate, as discussed above. The models proposed by Parkinson and the (6×3) model we proposed before for Ag(1 1 1) are shown in Fig. 5. We should note here that the expected diffraction peak positions of the unit cells proposed by Parkinson coincide with those of (6×3) model and just based on the helium diffraction it is very difficult to derive a definite conclusion regarding the true unit cell structure of pentacene monolayer on Au(1 1 1). In addition, even if different monolayer structures form, if their average domain size is not large enough, diffraction from these structures would produce only very broad peaks which could not be resolved in the diffraction pattern (see the discussion in experimental part). Nevertheless the plausibility of the (6×3) structure instead of the denser structures proposed by the other groups based on STM results can be discussed as follows. In the denser structures the pentacene molecules are very close to each other sideways such that if the molecules are arranged parallel (lying flat) to the surface (as shown in Fig. 5) then the hydrogen atoms would overlap. Hence, for such dense structures the molecules should be tilted to provide enough space between the molecules. However, many theoretical calculations on pentacene on Ag(1 1 1) and Au(1 1 1) suggest a flat lying molecules in the first layer to be more stable than tilted ones [20,22,23,27]. In addition, flat orientation was also suggested by NEXAFS results [9,13] and the (6×3) structure was observed by STM on Ag(1 1 1) [18] before. Finally, it should also be noted here that, the difference of growth conditions employed in this study and in the literature studies reported above may also have caused a different monolayer structure. As discussed above, here we used SMBD and 200 K substrate temperature, since in our past stud-

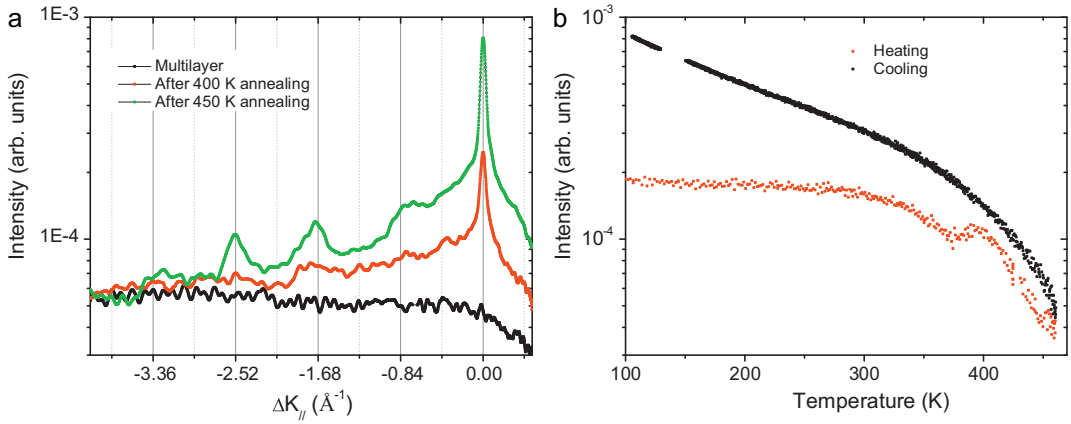

Fig. 4. (a) Diffraction scans of a 8 ML thick pentacene multilayer, along ⟨1 1 −2⟩ direction, on Au(1 1 1) grown with helium carrier gas and evolution of the diffraction pattern with annealing. (Due to very low scattering intensities of the multilayers caused by their poor quality, here data is presented after smoothing by adjacent point averaging for better viewing in logarithmic scale). (b) Helium SRI signal as a function of substrate temperature during heating and cooling of a 6 ML thick multilayer film grown with helium carrier gas.

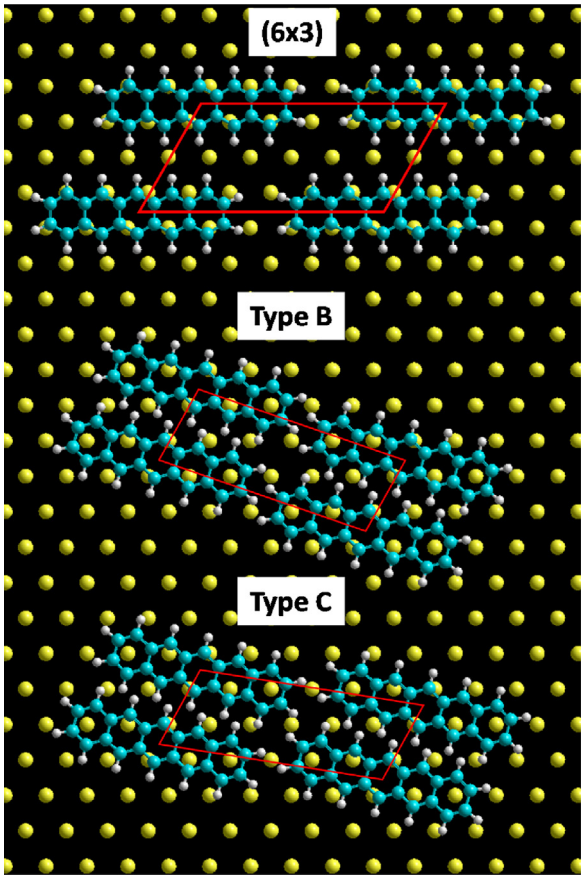

Fig. 5. Unit cell models for pentacene monolayer proposed here (6×3) and by Parkinson and co-workers "type B" and "type C". The models are not meant to depict the true adsorption site. In addition, in all the models pentacene molecules are shown lying flat on the surface which may not be the actual orientation of the molecules.

ies regarding pentacene on Ag(1 1 1) we observed 200 K to be the optimum substrate temperature for an ordered monolayer growth and above or below this temperature no significant change in the film structure was observed. However, in the works of Parkinson and co-workers and Kang and Zhu regular thermal evaporation was employed at 300 K substrate temperature. In addition, Parkinson and co-workers obtained their monolayer films by annealing higher coverage films (multilayers) at 333 K.

4. Conclusions

Here, we have reported the first surface diffraction measurements on pentacene thin films on Au(1 1 1). We have grown the pentacene thin films using SMBD and we were able to correlate helium SRI data to film thickness by simultaneously recording LEAD and QRFS data during film growth. For monolayer films diffraction patterns consistent with a (6×3) unit cell, which previously was also reported for Ag(1 1 1), was observed. There were no significant difference between the monolayers grown with helium and krypton carrier gasses. No ordered multilayer structures could be observed regardless of the type of the carrier gas. Desorption of the multilayers took place starting at 385 K in agreement with previous reports in the literature.

Acknowledgements

This work was supported by TUBITAK grant no. 209T084 and was partially supported by Scientific Research Projects Commission of Ahi Evran University (Project No.: PYO 4001 13 003).

References

[1] A. Facchetti, Mater. Today 10 (2007) 28–37.
[2] J.E. Anthony, Angew. Chem. Internat. Ed. 47 (2008) 452–483.
[3] J.A. Rogers, T. Someya, Y.G. Huang, Science 327 (2010) 1603–1607.
[4] A.C. Arias, J.D. MacKenzie, I. McCulloch, J. Rivnay, A. Salleo, Chem. Rev. 110 (2010) 3–24.
[5] R. Ruiz, et al., Chem. Mater. 16 (2004) 4497–4508.
[6] P.G. Schroeder, C.B. France, J.B. Park, B.A. Parkinson, J. Appl. Phys. 91 (2002) 3010–3014.
[7] C.B. France, P.G. Schroeder, J.C. Forsythe, B.A. Parkinson, Langmuir 19 (2003) 1274–1281.
[8] J.H. Kang, X.Y. Zhu, Appl. Phys. Lett. 82 (2003) 3248–3250.
[9] G. Beernink, T. Strunskus, G. Witte, C. Woll, Appl. Phys. Lett. 85 (2004) 398–400.
[10] M.F. Danisman, L. Casalis, G. Scoles, Phys. Rev. B 72 (2005) 9.
[11] J.H. Kang, X.Y. Zhu, Chem. Mater. 18 (2006) 1318–1323.
[12] L. Floreano, A. Cossaro, D. Cvetko, G. Bavdek, A. Morgante, J. Phys. Chem. B 110 (2006) 4908–4913.
[13] M. Pedio, et al., Appl. Surf. Sci. 254 (2007) 103–107.
[14] Y. Zheng, D.C. Qi, N. Chandrasekhar, X.Y. Gao, C. Troadec, A.T.S. Wee, Langmuir 23 (2007) 8336–8342.
[15] E. Annese, C.E. Viol, B. Zhou, J. Fujii, I. Vobornik, C. Baldacchini, M.G. Betti, G. Rossi, Surf. Sci. 601 (2007) 4242–4245.
[16] C. Baldacchini, F. Allegretti, R. Gunnella, M.G. Betti, Surf. Sci. 601 (2007) 2603–2606.
[17] M. Satta, S. Iacobucci, R. Larciprete, Phys. Rev. B 75 (2007).
[18] D.B. Dougherty, W. Jin, W.G. Cullen, J.E. Reutt-Robey, S.W. Robey, J. Phys. Chem. C 112 (2008) 20334–20339.
[19] H. Li, Y.Q. Duan, V. Coropceanu, J.L. Bredas, Org. Electron. 10 (2009) 1571–1578.
[20] E. Mete, I. Demiroglu, M.F. Danisman, S. Ellialtioglu, J. Phys. Chem. C 114 (2010) 2724–2729.
[21] E. Annese, I. Vobornik, G. Rossi, J. Fujii, Langmuir 26 (2010) 19142–19147.
[22] K. Toyoda, I. Hamada, K. Lee, S. Yanagisawa, Y. Morikawa, J. Chem. Phys. 132 (2010).
[23] W.D. Wheeler, B.A. Parkinson, Y. Dahnovsky, J. Chem. Phys. 135 (2011).
[24] B. Pieczyrak, E. Abad, F. Flores, J. Ortega, J. Chem. Phys. 135 (2011) 8.
[25] P. Clancy, Chem. Mater. 23 (2011) 522–543.
[26] S. Kawai, R. Pawlak, T. Glatzel, E. Meyer, Phys. Rev. B 84 (2011) 8.
[27] E. Mete, I. Demiroglu, E. Albayrak, G. Bracco, S. Elliatioglu, M.F. Danisman, J. Phys. Chem. C 116 (2012) 19429–19433.
[28] D. Kafer, L. Ruppel, G. Witte, Phys. Rev. B 75 (2007).
[29] L. Casalis, M.F. Danisman, B. Nickel, G. Bracco, T. Toccoli, S. Iannotta, G. Scoles, Phys. Rev. Lett. 90 (2003).
[30] E. Albayrak, M.F. Danışman, J. Phys. Chem. C (2013).
[31] M.F. Danisman, B. Ozkan, Rev. Sci. Instrum. 82 (2011).
[32] L. Bruschi, G. Delfitto, G. Mistura, Rev. Sci. Instrum. 70 (1999) 153–157.
[33] D.A. Buttry, M.D. Ward, Chem. Rev. 92 (1992) 1355–1379.
[34] D. Kafer, C. Woll, G. Witte, Applied, Phys. A Mater. Sci. Process. 95 (2009) 273–284.